Nanoscale

Accepted Manuscript

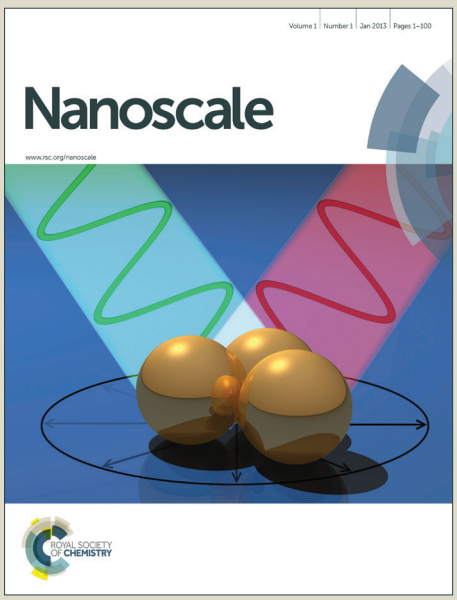

ROYAL SOCIETY OF CHEMISTRY

www.rsc.org/nanoscale

Nanoscale

RSCPublishing

COMMUNICATION

Highly reproducible SERS arrays directly written by inkjet-printing

Cite this: DOI: 10.1039/x0xx00000x

Qiang Yang,[fa,b] Mengmeng Deng,[fa] Huizeng Li,[a,b] Mingzhu Li,*[a] Cong Zhang,[a] Weizhi Shen,[a] Yanan Li,[a,b] Dan Guo,[a,b] and Yanlin Song*[a]

Received 00th January 2014,
Accepted 00th January 2014

DOI: 10.1039/x0xx00000x

www.rsc.org/

SERS arrays with uniform gold nanoparticles distribution were fabricated by direct-writing with inkjet printing method. Quantitative analysis based on Raman detection was achieved with a small standard statistical deviation of less than 4% for the reproducibility and that of less than 5% for the long-term stability for 12 weeks.

Surface enhanced Raman scattering (SERS) takes superior advantages of ultra-sensitive, non-destruction, low cost and real-time detection.[1] SERS has been one of the most powerful tools for molecular detection and has been an excellent probing tool for trace detection of a great variety of chemicals and biological samples, which has been spread widely in life care, environmental monitoring, food safety and security defense.[2] However, the poor reproducibility of SERS has hindered its development and application especially for the clinical and pharmaceutical detection.[3] In order to improve the reproducibility for SERS detection, fine structures were constructed by Focused Ion Beam Milling,[4] Electron-beam Lithography,[5] etching,[6] self-assembly,[7] laser induced photoreduction[8] and nanomanipulation[9]. For example, J. Wenger et al. fabricated a single nanogap with size of tens of nanometers in a concave box by milling of Focused Ion Beam, and achieved single molecule detection.[4] In addition, H. Misawa et al. prepared well-defined gold nanostructures by high-resolution electron beam lithography/lift-off techniques, and its SERS measurements showed high reproducibility.[5] Kim et al. fabricated an ultrahigh-density array of silver nanoclusters for SERS substrate with high sensitivity and excellent reproducibility at a very large area (wafer scale) based on polystyrene-block-poly(4-vinylpyridine) copolymer (PS-b-P4VP) micelles.[10] However, most of these techniques are complicated and expensive. [7-9, 11] It is still a great challenge for SERS application to compromise the balance between the facility of SERS-active substrates fabrication and the reproducibility of the SERS detection.[2a, 12]

In this work, we developed an alternative strategy using ink-jet printing to direct write on substrates to prepare SERS devices. Inkjet printing is an attractive technology to fabricate large-scale patterns or devices due to its advantages of low-cost, efficient use of materials and waste elimination.[13] Precisely controlling of the printing droplets can fabricate high-resolution patterns with versatile materials. Nevertheless, its application on SERS devices are restricted by inhomogeneous distribution of nanoparticles during droplet drying process, which greatly reduced its reproducibility. In this communication, the reproducibility of the SERS detection was enhanced by controlling the wettability of the substrates. As a result, the inkjet printed SERS-active spots on hydrophobic substrates exhibited homogeneous distribution and close packing of gold nanoparticles (AuNPs), which could enhance the Raman scattering of molecules due to the enhanced electromagnetic field between AuNPs under laser illumination.[2b, 14] Consequently, the SERS-active spots showed high reproducibility for the SERS detection with site to site enhancement factor variations smaller than 4%, as well as high sensitivity with detection limit low to 10^{-10} M. Moreover, the achieved SERS-active spots can be easily patterned and facilely fabricated in a large scale, which can realize rapid and mass quantitative analysis in chemical detection and biological diagnosis.

As showed in Fig. 1a, the SERS device was fabricated by inkjet printing ink of monodispersed AuNPs latex on a hydrophobic smooth substrate. The hydrophobic surface of silicon wafer, with contact angle (CA) of 117.6 ° **(**inset of Fig. 2c**),** was fabricated by modification of 1H, 1H, 2H, 2H-

perfluorodecyltriethoxysilane after being cleaned by piranha solution. On the hydrophobic surface, the receding of the triple phase line of inkjet printed droplets was able to eliminate the coffee ring effect.[15] As a result, the nanoparticles could be homogeneously distributed on the hydrophobic substrate. Additionally, the smooth surface, in contrast to the micro-nano structure for a superhydrophobic substrate, was helpful to drive the nanoparticles to self-assemble on the hydrophobic surface, which was crucial to obtain homogeneously distributed hot spots. In this communication, we prepared an array of SERS-active AuNPs spots (Fig. 1c). The Scanning Electron Microscopy (SEM) image in Fig. 1d showed that the inkjet printed AuNPs spot was uniform and the AuNPs were self-assembled into close-packed structure (inset of Fig. 1d). The uniform structure resulted from the retracting of triple phase contact line to contract the drop into the center, which drove the AuNPs to aggregate in the center and pack closely.[15a] Moreover, the well-monodispersed AuNPs, with size of 13.04 ± 1.47 nm (Fig. S1), were helpful to form homogeneously distributed hot spots, which contributed greatly to the enhanced reproducibility of the SERS detection. Additionally, It is worth mentioning that a hydrophilic-hydrophobic pattern could be achieved due to the AuNPs spot was hydrophilic (CA: 0 °) and the substrate was hydrophobic (CA: 117.6 °). Dripping an aqueous drop with analytes on the pattern, the target detection objects would be efficiently concentrated onto the AuNPs spots (Fig. 1b), which could enhance the accuracy of detection and overcome the diffusion limit of objects in many applications such as ultratrace detection.[6, 16]

In order to demonstrate the influence of wettability on the structure of the Raman-active AuNPs spot made by inkjet printing, the substrates with different wettability, with different contact angles (CAs) of 59.6 ± 1.3 ° for the hydrophilic substrates and 117.6 ± 1.1 ° for the hydrophobic substrates, were fabricated (insets of Fig. 2a and 2c). In this work, ink droplets of 10 pL were printed. The images in Fig. 2 showed that on substrates with different wettability, the distribution and assembly of AuNPs were definitely different. On the hydrophilic substrate (Fig. 2a), the triple phase contact line pinned on the periphery of the ink-jet print spots (inset of Fig. 2e and Fig. S4a). As the evaporation velocity of solvent at the periphery was faster than that inside the spot, the AuNPs would move toward and deposit on the periphery, which was called the coffee ring effect (Fig. 2b).[15a] Inside the rings, nevertheless, there were a few randomly scattered particles, which was attributed to the Marangoni effect.[17] The scattered AuNPs would do harm to the

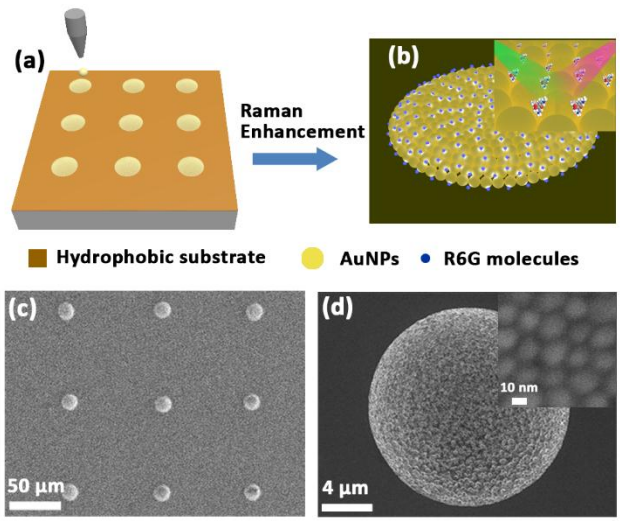

Fig. 1 Characterization of as-prepared SERS-active spots on hydrophobic substrates (contact angle: 117.6 ± 1.1 °). (a) An AuNPs array was inkjet printed on a hydrophobic substrate. (b) The analytes molecules were homegeneously distributed on the AuNPs array, and the inset shows the Raman light of the molecules was enhanced by the AuNPs. (c) SEM image of an array of AuNPs SERS-active spots printed on the hydrophobic substrate. (d) SEM image of an AuNPs SERS-active spot from above matrix. Inset shows the SEM image for characterizing the assembly of the surface AuNPs on the SERS-active spots which showed that their size was 13.04 ± 1.47 nm and the size of nanogaps was 4.16 ± 0.70 nm.

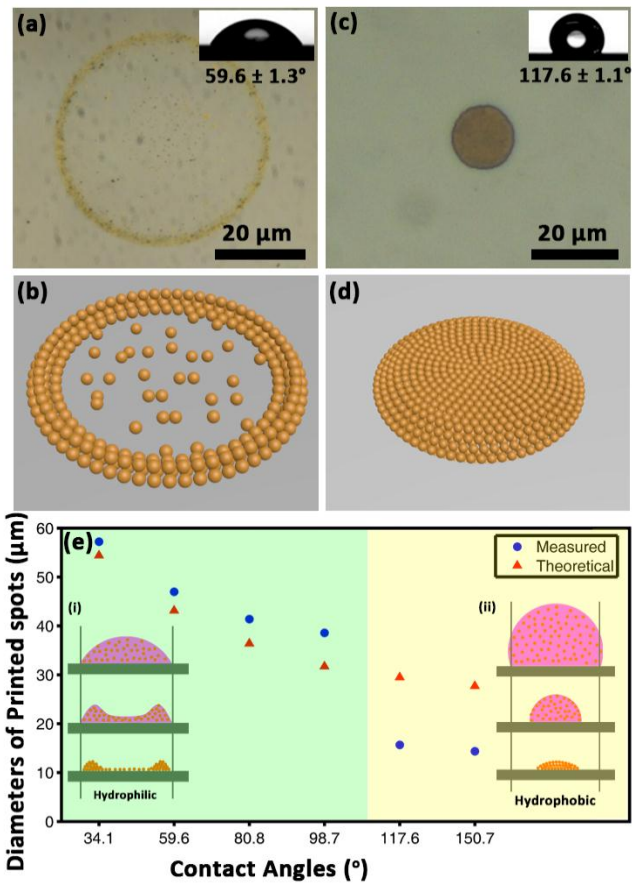

Fig. 2 Optical images (a, c) and corresponding schemtical illustration (b, d) of morphologies of inkjet print AuNPs ink droplets (5 wt%) after drying on hydrophilic (CA: 59.6 ± 1.3 °) and hydrophobic (CA: 117.6 ± 1.1 °) substrates, respectively. The insets show the wettability charaterization for the substrates with above contact angles, correspondingly.(e) the theoretically calculated and experimentally measured diameters of printed droplets with respected to different contact angles. The insets show the dewetting processes of droplets on the hydrophilic and hydrophobic substrates, respectively.

reproducibility of the SERS detection. For the hydrophilic substrate, in addition, the diameter of the droplet dropped on the substrate was 47.0 μm, which was larger than the theoretically calculated diameters (Equation 1) of 43.1 μm (Fig. 2e).

$$d_{hydrophilic} = \sqrt[3]{\frac{24Vsin^3\theta}{\pi(2+cos\theta)(1-cos\theta)^2}} \quad (1)$$

where d represents the diameter of the wetted area, V represents the volume of the droplet, which is 10 pL in this work, θ represents the contact angle of the droplet on a hydrophilic substrate. The calculation steps are demonstrated in the supporting information (Fig. S2 and S3). The larger spots were ascribed to the spreading of droplets when it impacted on the substrates during inkjet printing process. For the hydrophilic substrates with other contact angles, the formed spots were also larger than the theoretically calculated sizes (Fig. 2e), which indicated that the coffee rings were formed. On the hydrophobic substrates with CA of 117.6 °(Fig. 2c), however, the diameter of the printed spot on the substrate was 14.2 μm. The size was smaller than the theoretical calculated diameter (Equation 1) of 29.5 μm (Fig. 2e).

$$d_{hydrophilic} = \sqrt[3]{\frac{24V}{\pi\left(4-\frac{(2-cos\theta)(1+cos\theta)^2}{\sin^3\theta}\right)}} \quad (2)$$

The calculation steps are demonstrated in the supporting information (Fig. S2 and S3). The result suggested that the triple phase contact lines moved towards the center (inset of Fig. 2e and Fig. S4b), leading to the suppression of the coffee ring (Fig. 2d). As a result, the AuNPs were self-assembled into closed-packed structure and formed a homogeneously distributed AuNPs layer on the surface of the dried spot (Fig. 2c). Above all, the hydrophobic substrate was the priority for preparing a routine SERS device in this work.

To demonstrate the relationship of reproducibility of SERS detection with respect to the wettability of substrates, R6G molecules detection was achieved on them and the results were shown in Fig. 3. A 5 μL drop of R6G aqueous solution with concentration of 1×10^{-7} M was dropped on an AuNPs SERS-active spot. The strongest peaks at wavenumbers of 1509 cm^{-1}, 1359 cm^{-1} and 611 cm^{-1} at the Raman spectroscopy were selected to characterize quantity of R6G molecules. Nine inkjet spots were randomly selected for SERS signal measurement. The spectra curves achieved from the hydrophobic substrates were identical without significant deviation (Fig 3a). With statistical calculation, the relative standard deviations (RSD) at wavenumbers of 1509 cm^{-1}, 1359 cm^{-1} and 611 cm^{-1} were 3.60%, 3.37% and 2.60%, respectively. Among the three band peaks, the peak intensities maintained within 4%, which indicated the high reproducibility of inkjet-printed microarray of SERS-active spots for Raman spectroscopy.[3d, 18] In comparison, the spectra curves achieved from the hydrophilic substrates showed significant deviation (Fig 3b). The RSD at wavenumbers of 1509 cm^{-1}, 1359 cm^{-1} and 611 cm^{-1} were 27.4%, 20.8% and 27.7%, respectively. The big RSD values were ascribed to the non-uniform distribution of AuNPs on the hydrophilic substrates. Another phenomenon should be mentioned that, the analytes could be concentrated on the hydrophilic SERS-active spot due to the wettability difference between as-prepared hydrophilic spot and the hydrophobic substrate, which could break the

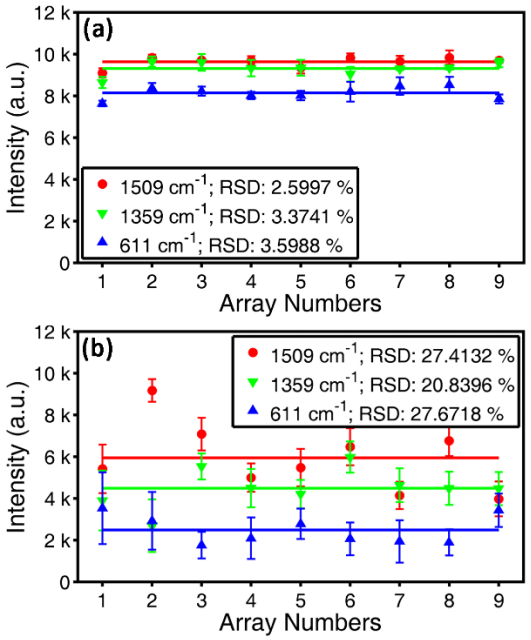

Fig. 3 Comparison of reproducibility for SERS detection on substrates with different wettability. SERS intensities and their average lines at wavenumbers of 1509 cm^{-1}, 1359 cm^{-1} and 611 cm^{-1} for R6G with concentration of 1×10^{-7} M concerning to different array spots, with at least 5 sites for SERS detection in each spot, on the hydrophobic (a) and hydrophilic (b) substrates.

diffusion limit existed in traditional immersing method and improve the detection limit. The SERS signal intensities achieved from the hydrophobic substrates were 1.62, 2.08, 3.28 times larger than that from the hydrophilic ones, corresponding to the wavenumbers of 1509 cm^{-1}, 1359 cm^{-1} and 611 cm^{-1}, respectively. The enhanced sensitivity was attributed to the concentration effect for R6G molecules on the hydrophobic substrates.

With the superior reproducibility of SERS detection on the hydrophobic substrates, the sensitivity, correlation and detection limit, which were essential for a practical analysis method, were characterized and obtained (Fig. 4). The SERS spectra exhibited in Fig. 4a were attained with R6G concentration ranging from 1×10^{-4} M to 1×10^{-10} M. With wavenumbers of 611 cm^{-1}, 1359 cm^{-1} and 1509 cm^{-1} at the Raman spectroscopy identified the R6G, the intensity with respect to the logarithms of R6G concentration was plot in Fig. 4b. The three plots showed well linearity. According to the fitted lines, the fitted equations at wavenumbers of 611 cm^{-1}, 1359 cm^{-1} and 1509 cm^{-1} were $I_{611} = 36955.4 + 4134.1 \log(C_{R6G})$, $I_{1359} = 50255.0 + 5703.2 \log(C_{R6G})$ and $I_{1509} = 55027.9 + 6241.5 \log(C_{R6G})$, respectively. The data was well-fitted linearly. Their large correlation coefficients are 0.9873, 0.9897 and 0.9925 corresponding to peaks at wavenumbers of 611 cm^{-1}, 1359 cm^{-1} and 1509 cm^{-1}, respectively. Moreover, the detect limit of the printed SERS substrates, shown in the inset of Fig. 4a, was 10^{-10} M (4.79 ppb). The results indicated that the SERS substrates were able to be used to be a practical analysis method. In addition, the stability of the hydrophobic substrate

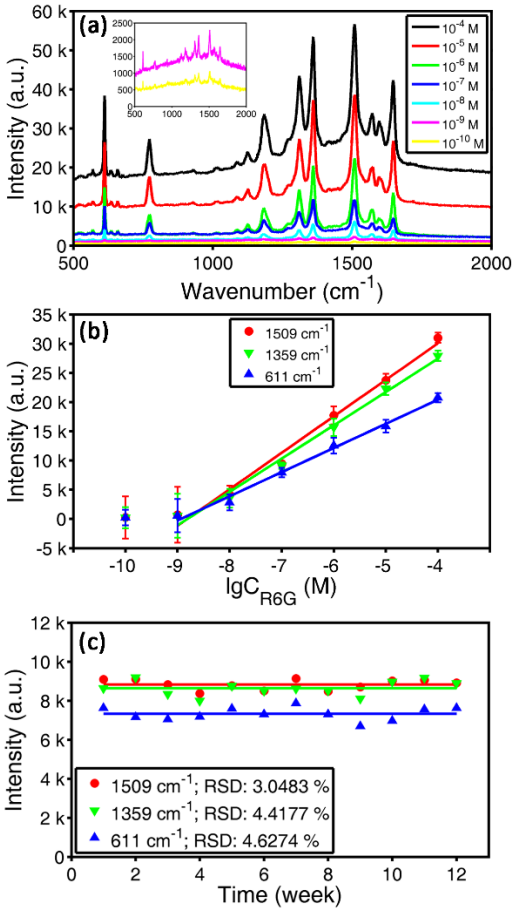

Fig. 4 (a) SERS spectra of rhodamine 6G (R6G) in AuNPs microarrays on hydrophobic substrates (contact angle: *ca.*117.6 °) with a series of concentration ranging from 1 × 10^{-4} M to 1 × 10^{-10} M. (b) SERS intensities and their linear fitted lines at wavenumbers of 1509 cm^{-1}, 1359 cm^{-1} and 611 cm^{-1} with respect to above concentration of R6G. The error bars represent relative standard deviations and were obtained with at least 5 repeated trials**.** (c) SERS intensities at wavenumbers of 1509 cm^{-1}, 1359 cm^{-1} and 611 cm^{-1} for R6G with concentration of 1 × 10^{-7} M as a function of time during 12 weeks.

was also characterized in Fig. 4c. During 12 weeks, the average SERS intensities at the wavenumbers of 611 cm^{-1}, 1359 cm^{-1} and 1509 cm^{-1} for R6G molecules were obtained. Moreover, the RSD for the three wavenumbers were 3.05%, 4.42% and 4.63%, corresponding to the wavenumbers at 611 cm^{-1}, 1359 cm^{-1} and 1509 cm^{-1}, respectively. The results indicated that the sample was very stable. The results further indicated that the SERS microarray was able to be a practice and applicable analysis method.

Conclusions

In conclusion, a SERS-active spot array with high reproducibility was fabricated by inkjet printing-assisted self-assembly of the monodispersed AuNPs. The as-prepared SERS-active spot exhibited excellent reproducibility with RSD smaller than 4%, long-term stability with RSD smaller than 5%. Moreover, the detection limits of the microarray sensor about 5 ppb, which was better than a standard colloidal method. The as-prepared SERS-active patterns were universal for the Raman detection which could achieve high reproducibility, long-term stability, and excellent sensitivity and accuracy. Moreover, the fabrication strategy was fast, low-cost, and of capability for large scale preparation. We anticipate that the strategy and as-prepared SERS-active pattern will be of great potential for the chemical sensor and biology diagnosis.

Acknowledgement

This work is supported by the National Nature Science Foundation NSFC (No. 51173190, 21003132, 91127038, and 21121001), the 973 Program (No. 2013CB933004, 2011CB932303, and 2011CB808400), Beijing Nova Program (No. Z131103000413051), and the "Strategic Priority Research Program" of the Chinese Academy of Sciences (No. XDA09020000).

Notes and references

[a] *Key Laboratory of Green Printing, Beijing National Laboratory for Molecular Sciences (BNLMS), Center for Molecular Sciences, Institute of Chemistry, Chinese Academy of Sciences, Beijing 100190, P. R. China E-mail: ylsong@iccas.ac.cn; mingzhu@iccas.ac.cn*
[b] *University of Chinese Academy of Sciences, Beijing, 100190, P.R. China.*
[£] *These authors contributed equally to this work.*

†See DOI: 10.1039/b000000x/
Electronic Supplementary Information (ESI) available: Additional information on the experimental details, gold nanoparticles characterization, and theoretical calculation for the diameters of contact area of droplets on substrates with different contact angles. See DOI: 10.1039/c000000x/

1 a) Z. Huang, G. Meng, Q. Huang, Y. Yang, C. Zhu and C. Tang, *Adv. Mater.*, 2010, **22**, 4136; b) W. Lee, S. Y. Lee, R. M. Briber and O. Rabin, *Adv. Funct. Mater.*, 2011, **21**, 3424; c) G. Braun, S. J. Lee, M. Dante, T.-Q. Nguyen, M. Moskovits and N. Reich, *J. Am. Chem. Soc.*, 2007, **129**, 6378; d) M. D. Porter, R. J. Lipert, L. M. Siperko, G. Wang and R. Narayanan, *Chem. Soc. Rev.*, 2008, **37**, 1001; e) A. Sassolas, B. D. Leca-Bouvier and L. J. Blum, *Chem. Rev.*, 2007, **108**, 109.
2 a) B.-B. Xu, Y.-L. Zhang, W.-Y. Zhang, X.-Q. Liu, J.-N. Wang, X.-L. Zhang, D.-D. Zhang, H.-B. Jiang, R. Zhang and H.-B. Sun, *Adv. Opt. Mater.*, 2013, **1**; b) J. F. Li, Y. F. Huang, Y. Ding, Z. L. Yang, S. B. Li, X. S. Zhou, F. R. Fan, W. Zhang, Z. Y. Zhou, D. Y. Wu, B. Ren, Z. L. Wang and Z. Q. Tian, *Nature*, 2010, **464**, 392; c) L. Zhang, W. F. Dong, Z. Y. Tang, J. F. Song, H. Xia and H. B. Sun, *Opt. Lett.*, 2010, **35**, 3297.
3 a) L. Wu, Z. Wang and B. Shen, *Nanoscale*, 2013, **5**, 5274; b) O. Peron, E. Rinnert, T. Toury, M. L. de la Chapelle and C. Compere, *Analyst*, 2011, **136**, 1018; c) L. Rodriguez-Lorenzo, L. Fabris and R. A. Alvarez-Puebla, *Anal. Chim. Acta*, 2012, **745**, 10; d) S. Mabbott, I. A. Larmour, V. Vishnyakov, Y. Xu, D. Graham and R. Goodacre, *Analyst*, 2012, **137**, 2791.
4 D. Punj, M. Mivelle, S. B. Moparthi, T. S. van Zanten, H. Rigneault, N. F. van Hulst, M. F. Garcia-Parajo and J. Wenger, *Nat. Nanotechnol.*, 2013, **8**, 512.
5 Y. Yokota, K. Ueno and H. Misawa, *Small*, 2011, **7**, 252.
6 F. De Angelis, F. Gentile, F. Mecarini, G. Das, M. Moretti, P. Candeloro, M. L. Coluccio, G. Cojoc, A. Accardo, C. Liberale, R. P. Zaccaria, G. Perozziello, L. Tirinato, A. Toma, G. Cuda, R. Cingolani and E. Di Fabrizio, *Nat. Photonics*, 2011, **5**, 683.
7 F. L. Yap, P. Thoniyot, S. Krishnan and S. Krishnamoorthy, *ACS Nano*, 2012, **6**, 2056.
8 B.-B. Xu, Z.-C. Ma, L. Wang, R. Zhang, L.-G. Niu, Z. Yang, Y.-L. Zhang, W.-H. Zheng, B. Zhao, Y. Xu, Q.-D. Chen, H. Xia and H.-B. Sun, *Lab Chip*, 2011, **11**, 3347.
9 L. Zhang, T. Li, B. Li, J. Li and E. Wang, *Chem. Commun.*, 2010, **46**, 1476.

10 W. J. Cho, Y. Kim and J. K. Kim, *ACS Nano*, 2012, **6**, 249.
11 a) M.-L. Seol, J.-H. Kim, T. Kang, H. Im, S. Kim, B. Kim and Y.-K. Choi, *Nanotechnol.*, 2011, **22**, 235303; b) H. Wang, X. M. Han, X. M. Ou, C. S. Lee, X. H. Zhang and S. T. Lee, *Nanoscale*, 2013, **5**, 8172; c) Z. Li, W. Ruan, W. Song, X. Xue, Z. Mao, W. Ji and B. Zhao, *Spectrochim. Acta, Part A*, 2011, **82**, 456.
12 R. Zhang, B. B. Xu, X. Q. Liu, Y. L. Zhang, Y. Xu, Q. D. Chen and H. B. Sun, *Chem. Commun.*, 2012, **48**.
13 J. Park, J. Moon, H. Shin, D. Wang and M. Park, *J. Colloid Interface Sci.*, 2006, **298**, 713.
14 Y. Tang and M. Ouyang, *Nat. Mater.*, 2007, **6**, 754.
15 a) M. Kuang, J. Wang, B. Bao, F. Li, L. Wang, L. Jiang and Y. Song, *Adv. Opt. Mater.*, 2014, **2**, 34; b) Z. Zhang, X. Zhang, Z. Xin, M. Deng, Y. Wen and Y. Song, *Adv. Mater.*, 2013, **25**, 6714.
16 J. Hou, H. C. Zhang, Q. Yang, M. Z. Li, Y. L. Song and L. Jiang, *Angew. Chem., Int. Ed.*, 2014, **53**, 5791.
17 H. Hu and R. G. Larson, *J. Phys. Chem. B*, 2006, **110**, 7090.
18 L.-Q. Lu, Y. Zheng, W.-G. Qu, H.-Q. Yu and A.-W. Xu, *J. Mater. Chem.*, 2012, **22**, 20986.